Powder Metallurgy Progress, Vol.18 (2018), No.1, p.021-030
http://dx.doi.org/10.1515/pmp-2018-0003

SURFACE HARDENING VS. SURFACE EMBRITTLEMENT IN CARBURIZING OF POROUS STEELS

S. Tesfaye Mekonone, I. Cristofolini, W. Pahl, A. Molinari

Abstract

Carburizing increases the contact fatigue resistance of sintered steels, but the surface hardening may result the formation of surface brittle cracks due to the combined effect of high hardness and porosity. The effect of carburizing on the embrittlement of the case of a 7.3 g/cm^3 1.5%Mo - 0.25%C sintered steel was studied. The phenomenon was analyzed theoretically and verified by experiments. The resistance of the carburized steel to surface brittle cracking increases with the load bearing surface and the decrease of the maximum pore size, of the surface microhardness and the friction coefficient. The theoretical analysis was implemented in a design procedure for parts subject to contact stresses.

Keywords: Carburizing, rolling-sliding, hardening; brittleness; design

INTRODUCTION

In lubricated rolling and rolling-sliding contacts, the main damage mechanism is contact fatigue that occurs through the nucleation of a subsurface crack, its propagation towards the surface and the formation of metallic debris. The resistance of porous sintered steels to this damage mechanism has been investigated in previous works, proposing a theoretical model to predict the nucleation of the subsurface crack [1-2]. The model is based on a conservative approach, starting from the assumption that crack nucleation is anticipated by local plastic deformation [3]. Therefore, if the resistance to plastic deformation of the matrix is higher than the maximum local stress, no plastic deformation occurs and, in turn, subsurface cracks do not nucleate.

The resistance to plastic deformation of the matrix σ_{yo} can be calculated from microhardness HV by eq. (1) [4], while the maximum local stress σ can be calculated from the equivalent stress σ_{eq} by eq. (2) [5].

$$\sigma_{yo} = \frac{HV}{4.2} \tag{1}$$

$$\sigma = \frac{\sigma_{eq}\beta_k}{\phi} \tag{2}$$

where β_k is the notch effect coefficient (2.4 for heat treated steels [6]) and Φ is the fraction of the load bearing section that may be determined from the fractional porosity and its morphology [7]. A detailed description of the theoretical model is reported in [2].

S. Tesfaye Mekonone, Ilaria Cristofolini, Alberto Molinari, University of Trento, Trento - Italy
Wolfgang Pahl, GKN SinterMetals, Brunico (BZ) - Italy

Figure 1 shows, as an example, a graphical representation of this model in case of a through hardened steel. It compares the yield strength of the matrix corresponding to different microhardness levels to the maximum stress profile corresponding to different fraction of the load bearing section, in specific contact conditions (curvature radii of the counteracting parts, contact length, contact force), just to highlight the influence of the microstructural characteristics of the sintered steel.

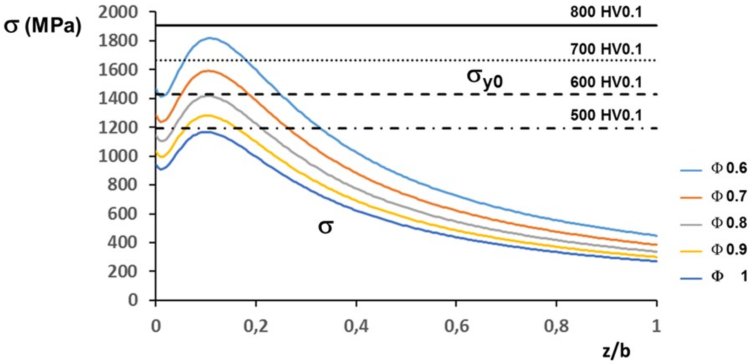

Fig.1. Yield strength of the matrix and maximum stress profile highlighting the conditions that cause subsurface plastic deformation.

For any fraction of the load bearing section, there is a minimum microhardness to avoid the nucleation of the subsurface crack. On decreasing the fraction of the load bearing section, the matrix microhardness has to be increased. This leads to a highly risky situation, since it has been demonstrated that pores may act as pre-existing cracks above a microhardness threshold, promoting brittle behavior [8].

Carburizing is a thermochemical treatment widely used for parts subject to fatigue and wear in application. Surface hardening is obtained through the carbon enrichment of the surface layers up to the eutectoidic composition and the heat treatment, which form a stress relieved martensitic case. Due to the high carbon content, the surface microhardness is usually greater than that of through hardened steels. In some conditions, the benefits deriving from the surface hardening may be eliminated by the embrittlement. In this work, the results of lubricated rolling-sliding tests of a carburized 1.5% Mo steel are presented, discussing the conditions that may cause brittle cracking of the surface. A theoretical analysis is also proposed, and introduced in a design methodology to select the material characteristics for the lubricated rolling-sliding and rolling-sliding wear.

EXPERIMENTAL PROCEDURE

The powder used for the production of the specimens is the 1.5% Mo prealloyed iron, to which 0.3% graphite was added. Rings with 16 mm internal diameter, 40 mm external diameter and 10 mm height were cold compacted and sintered at 1150°C in endogas. The sintered density is 7.3 g/cm^3. Gas carburizing in endogas and stress relief at 180°C in air were carried out.

Lubricated rolling-sliding tests were carried out on an Amsler tribometer, using the Castrol edge 5W-30 oil as lubricant. The counterface rings were made of the 1%C and 1.5%Cr bearing steel hardened at 62 HRc. 10% sliding was obtained by setting the rotation speed of the specimen and the counterface at 400 rpm and 360 rpm, respectively. The friction coefficient was continuously recorded during the tests. Tests were run up to one million of cycles and the formation of cracks was investigated by the metallographic analysis of the worn specimens.

RESULTS AND DISCUSSION

Figure 2 shows the microstructure of the case and of the bulk of the carburized steel. The surface microstructure is martensitic, with some retained austenite, while the core is bainitic.

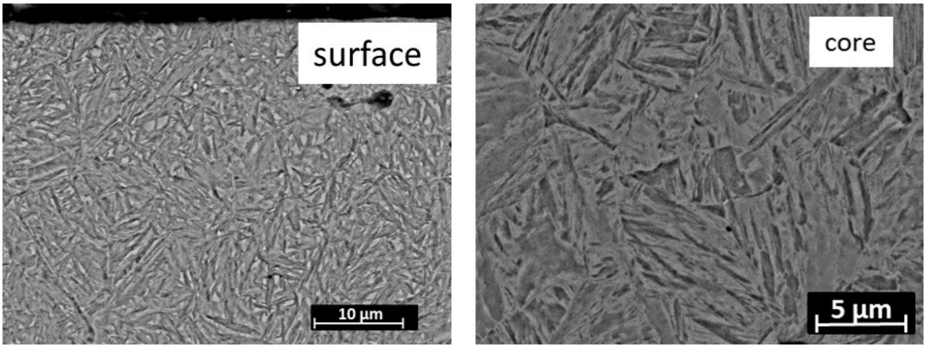

Fig.2. Microstructure of the carburized steel.

Figure 3 shows the microhardness profile of the carburized steel (left) and the results of the theoretical prediction of the resistance to the formation of subsurface cracks.

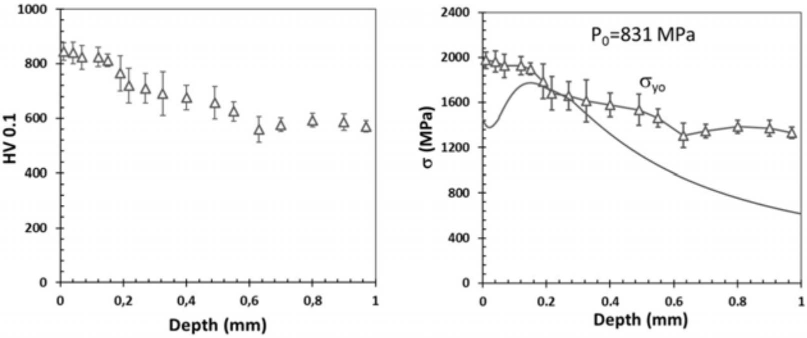

Fig.3. Microhardness profile of the carburized steel (left) and comparison between yield strength of the matrix and equivalent stress corresponding to 831 MPa mean Hertzian pressure.

From the microhardness profile (left plot) the profile of the yield strength of the matrix was calculated (line connecting the triangles in the right plot), and the maximum stress profile tangent to the yield strength one was determined (continuous line). The corresponding mean Hertzian pressure is 831 MPa. To verify the theoretical prediction, lubricated rolling-sliding tests were carried out at two mean pressures: 800 MPa and 850 MPa [9]. The metallographic analysis of the worn specimens shown subsurface cracks in the specimen tested at the higher mean pressure and no cracks in the other one, confirming the theoretical prediction. However, some cracks were observed in the surface layers of the latter, as those shown in Fig.4.

In particular the crack on the left side, perpendicular to the surface, can be attributed to a brittle damage caused by the tensile surface stress.

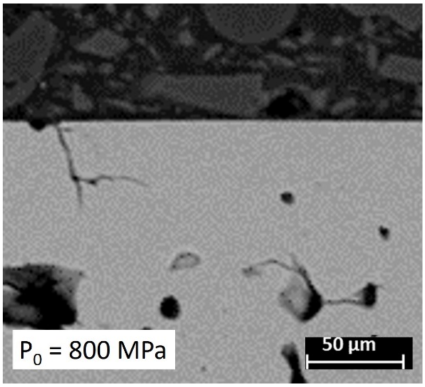

Fig.4. Example of brittle cracks in the surface layers of the worn carburized specimen.

The formation of a surface brittle crack occurs when the surface tensile stress σ_t exceeds the resistance of the material to the brittle fracture σ_f.

With reference to figure 5, the surface tensile stress is the tangential one along direction x. It is strongly dependent on the friction coefficient, as shown in the figure right, where the normalized tangential stress is plotted for three different values of μ.

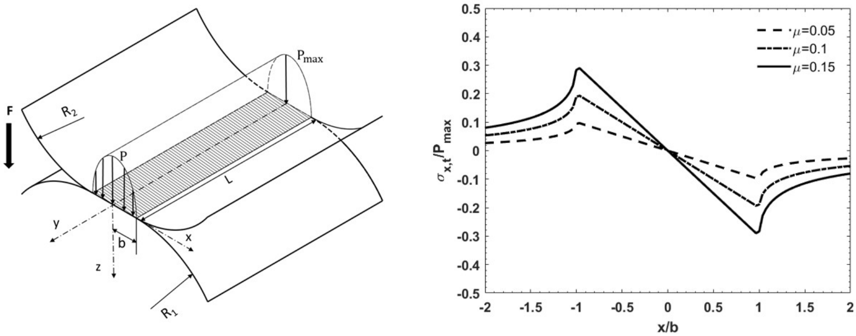

Fig. 5. Schematic representation of the contact pressure and effect of the friction coefficient on the normalized tangential stress.

The maximum tensile stress σ_t can be determined through equation (3)

$$\sigma_t = \frac{2P_{\max}\beta_k\mu}{M_{r2}} \tag{3}$$

where P_{max} is the maximum Hertzian pressure, μ is the friction coefficient and M_{r2} is the load bearing surface determined from the Abbott-Firestone diagram [10]. It is 0.85 for the carburized disks of the present investigation. The dependence of the tensile stress on M_{r2} and on the friction coefficient for different values of the mean Hertzian pressure P_0 (= 0.78 P_{max}) is shown in Fig.6.

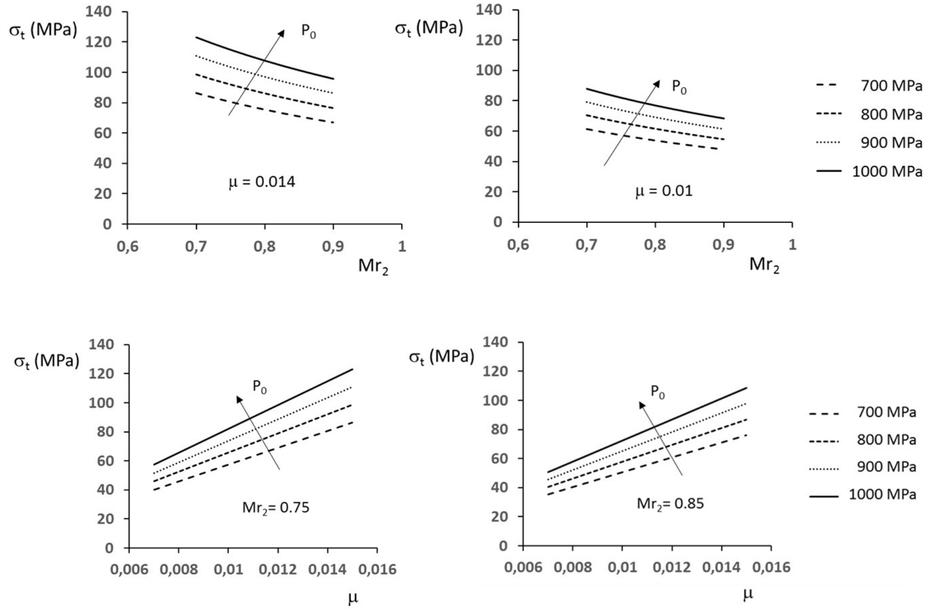

Fig.6. Surface tensile stress as a function of the load bearing surface (upper) and of the friction coefficient (lower) for different values of the mean Hertzian pressure.

The load bearing surface and the friction coefficient were varied within reasonable ranges in practical applications. The figure shows that friction coefficient has a great effect: even small variations may lead to a significant increase of the tensile stress.

The fracture stress is given by equation (4)

$$\sigma_f = \frac{K_{IC}}{\psi\sqrt{\pi\alpha}} \tag{4}$$

where K_{IC} is the fracture toughness of the matrix, Ψ is a geometrical parameter and *a* is the defect size. The fracture toughness may be determined by the yield strength of the matrix through eq. (5) [8]

$$K_{IC} = \frac{6000}{\sigma_{yo} + 300} \tag{5}$$

The defect size is the dimension of the larger pore on the surface. It may be measured by Image Analysis, that returns different parameters relevant to the pore size. Figure 7 shows two examples of the large pores observed on the specimen surface: the original image, the digitalized one and two parameters, the equivalent diameter D_{eq} and the maximum Feret diameter D_{max}.

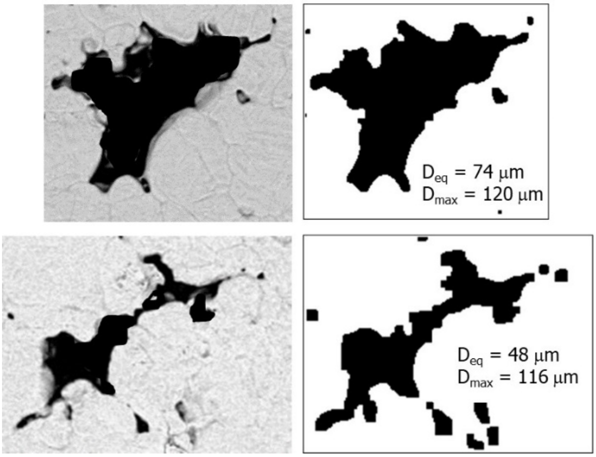

Fig.7. Examples of the large surface pores with equivalent diameter D_{eq} and maximum Feret diameter D_{max}.

The equivalent diameter is the diameter of the circle having the same area of the pore. It underestimates the effect of the pore on the crack propagation when pores are elongated as those in the figure. Therefore, the half of the maximum Feret diameter was taken as representative of the defect size in eq. (4).

Figure 8 shows the effect of the defect (pore) size and microhardness on σ_f.

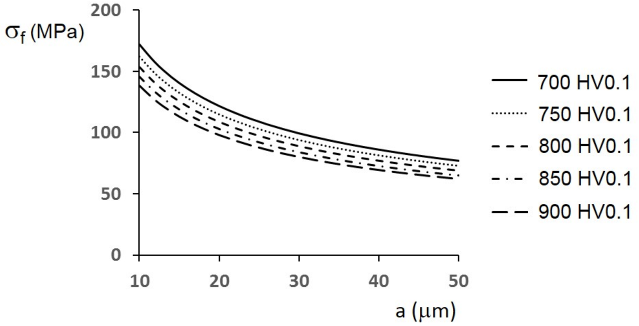

Fig.8. Effect of the defect (pore) size and microhardness on σ_f.

The resistance of the material to the propagation of the brittle fracture decreases with microhardness, due to the decrease of the fracture toughness, and with the pore size.

By combining equations (3) and (5) an expression for the critical pore size may be obtained, as by eq. (6).

$$\alpha = \frac{1}{4\psi^2\pi} K_{IC}^2 \left(\frac{M_{r2}}{\beta_k}\right)^2 \left(\frac{1}{\mu P_{\max}}\right)^2 \qquad (6)$$

It represents the minimum pore size that causes brittle cracking on the surface under the tensile stress.

Figure 9 shows the effect of the mean pressure and the friction coefficient on the critical pore size for a constant load bearing surface and two different microhardness values.

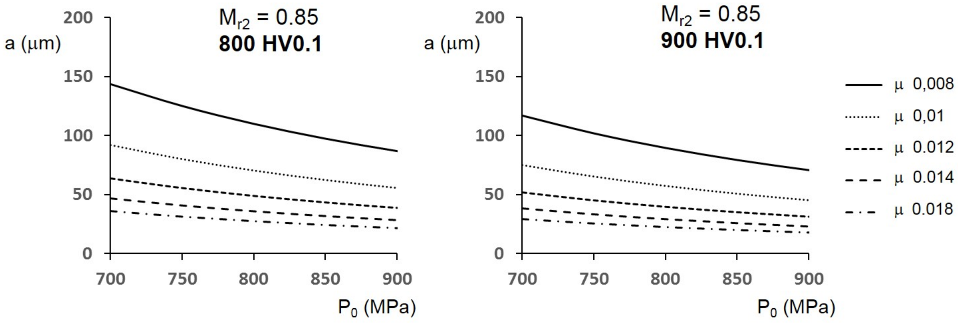

Fig.9. Effect of the mean pressure and the friction coefficient on the critical pore size.

This kind of diagram may be used to discuss the experimental evidence above described. Considering that:

- the maximum Feret diameter of the surface pores is 120 μm, that results in a defect size of 60 μm;
- the friction coefficient recorded during the tests at 800 MPa and 850 MPa mean pressure is 0.014;
- the surface microhardness of the carburized steel is 830 HV0.1;

Figure 10 shows that at 831 MPa mean pressure (the theoretical resistance to the formation of subsurface fatigue cracks) the formation of brittle cracks is predicted by the theoretical model.

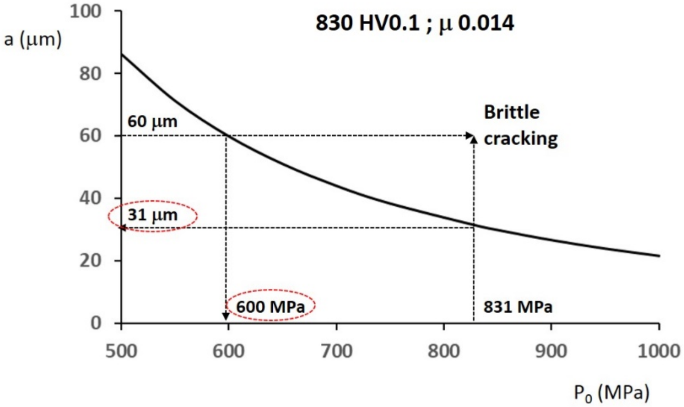

Fig.10. Theoretical prediction of the occurrence of brittle surface cracks in the carburized ring: effect of the pore size and the mean Hertzian pressure.

The brittle cracks are also expected at 800 MPa mean pressure, as observed experimentally. The figure also indicates that a maximum defect size of 31 μm, corresponding to a maximum Feret diameter of 62 μm, should prevent the formation of brittle cracks at 831 MPa. Such a maximum pore size could be obtained either strongly reducing the particle size or further increasing density, but both solutions are not practicable. The two real options are therefore surface densification and shot peening; the former reduces pore size dramatically, the latter introduces surface compressive residual stresses [9]. The material with the combination of the measured maximum Feret diameter and microhardness shown above would resist to the surface brittle cracking at a mean pressure of 600 MPa.

The resistance to brittle fracture may be increased through the fracture toughness by reducing microhardness. Figure 11 shows that microhardness should be decreased down to 560 HV0.1 to prevent brittle damage, but the resistance to the subsurface plastic deformation and fatigue crack nucleation would be seriously impaired.

Finally, the effect of the efficiency of lubrication is shown in Fig.12.

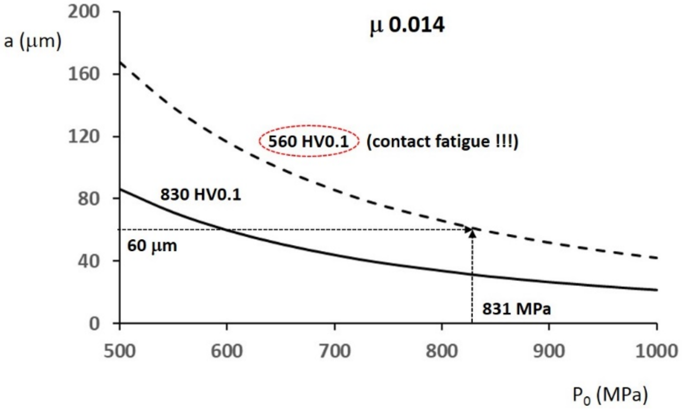

Fig.11. Theoretical prediction of the occurrence of brittle surface cracks in the carburized ring: effect of the surface microhardness.

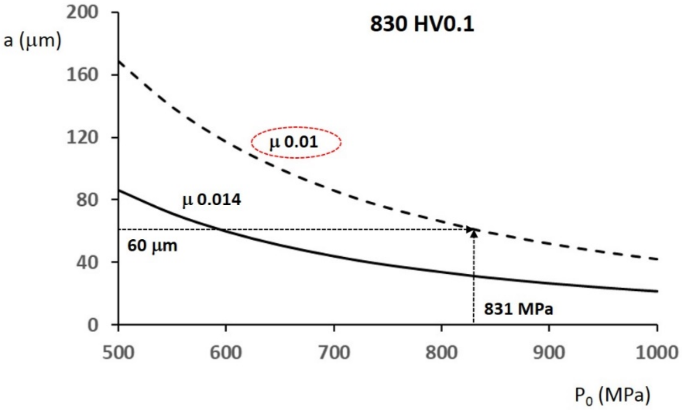

Fig.12. Theoretical prediction of the occurrence of brittle surface cracks in the carburized ring: effect of the friction coefficient.

The carburized steel with the measured maximum Feret diameter and microhardness shown above is expected to survive to brittle surface cracking if the friction coefficient is kept below 0.01. This indication confirms the great effect of the friction coefficient, and the importance to control the efficiency of lubrication.

All the theoretical work here presented may be implemented in the design procedure shown in Fig. 13.

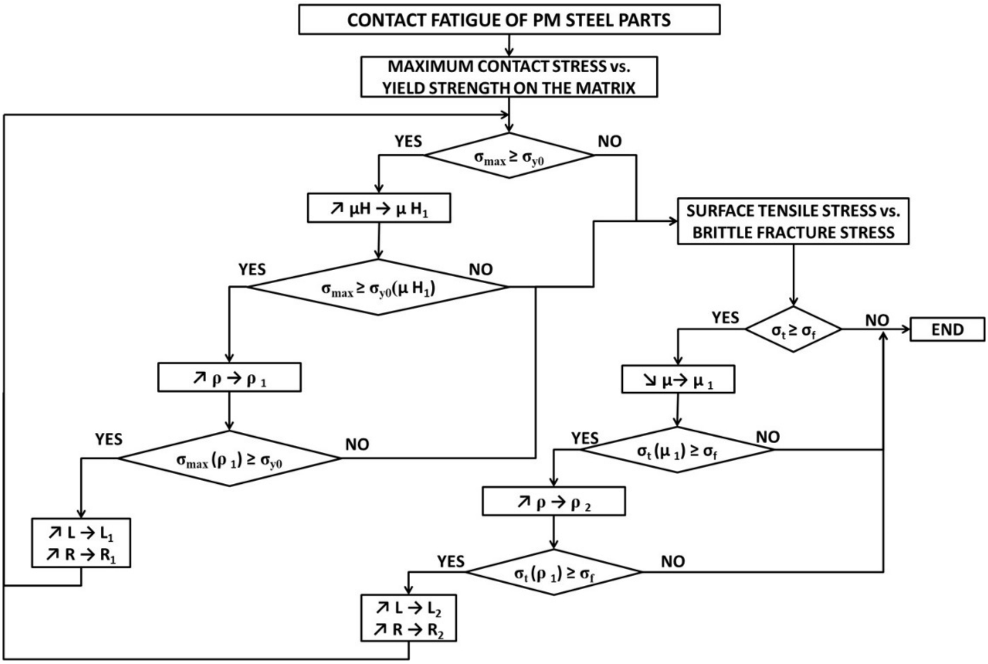

Fig.13. Design procedure for lubricated rolling and rolling-sliding.

The procedure starts checking the occurrence of the subsurface plastic deformation. If the maximum stress is greater than the yield strength of the matrix, a subsurface crack is expected to nucleate. Three possible solutions are sequentially verified:

- the increase in microhardness to increase the yield strength of the matrix;
- the increase in density to decrease the maximum contact stress;
- the change of the geometry of the parts, either increasing the contact radii or the contact length.

If the yield strength of the matrix results greater than the maximum contact stress either at the first verification or after the implementation of the three possible solutions, the nucleation of subsurface fatigue cracks will be prevented. The verification of the surface brittle cracking is then carried out.

If the tensile stress is greater than the resistance to brittle fracture of the material, the possible solutions are, in sequence:

- the control of the lubrication conditions, to reduce the friction coefficient;
- the increase in density to reduce the maximum pore size;
- the change of the geometry of the sintered part, to reduce the mean Hertzian pressure.

If the resistance to brittle fracture of the material results greater than the tensile stress either at the first verification or after the implementation of the three possible solutions, surface brittle cracking will be prevented.

CONCLUSION

The lubricated rolling-sliding behavior of a 7.3 g/cm^3 carburized 1.5%Mo - 0.25%C sintered steel was studied to verify the possible formation of surface brittle cracks due to the combined effect of the high surface microhardness and large surface pores. The resistance to the subsurface fatigue crack nucleation (contact fatigue) was determined in a previous work, resulting in a mean Hertzian pressure of 831 MPa. Tests at 800 MPa did not cause any subsurface cracking, but some surface cracks were observed in the worn specimens, attributable to a brittle behavior. Such a damage limits/eliminates the effect of carburizing on the resistance of the steel to contact fatigue.

The phenomenon was analyzed theoretically comparing the surface tensile stress to the fracture stress of the material. The resistance of the carburized steel to surface brittle cracking increases by increasing the load bearing surface and by decreasing the maximum pore size, the surface microhardness and the friction coefficient. In particular this last parameter plays a crucial role, since it greatly affects the surface tensile stress. Indeed, the decrease of the friction coefficient from 0.014 down to 0.01 increases the resistance to surface brittle cracking of the investigated material from 600 MPa to 831 MPa mean Hertzian pressure.

The theoretical analysis was implemented in a design procedure for parts subject to contact stresses, aiming at selecting the material and its heat treatment for a specific application, where contact stresses may cause both contact fatigue and brittle surface cracking.

REFERENCES

[1] Metinoz, I., Cristofolini, I., Pahl, W., Molinari, A.: Materials Science and Engineering A, vol. 614, 2014, p. 81
[2] Molinari, A., Metinoz, I., Cristofolini, I.: Powder Metallurgy Progress, vol. 14, 2014, n.1, p. 32
[3] Donzella, G., Petrogalli, C.: International Journal of Fatigue, vol. 32, 2010, p. 256
[4] Bell, T., Sun, Y.: Surface Engineering, vol. 6, 1990, p.133
[5] Tesfaye, S., Molinari, A., Pahl, W.: Powder Metallurgy, vol. 60, 2017, p. 231
[6] Pohl, D.: Powder Metallurgy International, vol. 1, 1969, p. 26
[7] Molinari, A., Menapace, C., Santuliana, E.: Powder Metallurgy Progress, vol. 11, 2011, p. 12
[8] Straffelini, G., Menapace, C., Molinari, A.: Powder Metallurgy, vol. 45, 2002, n. 2, p. 167
[9] Tesfaye, S., Molinari, A., Pahl, W., Denicolo, A., Marconi, P.: Advances in Powder Metallurgy & Particulate Materials, vol. 6, 2017, p. 589
[10] Cristofolini, I., Cipolloni, G., Molinari, A.: Advances in powder Metallurgy and Particulate Materials, vol. 2, 2012, p. 47